


 Cite this: *RSC Adv.*, 2022, 12, 19554

Two-photon absorption of 28-hetero-2,7-naphthiporphyrins: expanded carbaporphyrinoid macrocycles†

 Emma Robbins,^{ab} Radostaw Deska,^a Katarzyna Ślusarek,^c Marta Dudek,^a Marek Samoć,^a Lechosław Latos-Grażyński,^c Bartosz Szyszko^{bc*} and Katarzyna Matczyszyn^{ba}

The one- and two-photon absorption (1PA and 2PA) properties of three expanded aceneporphyrinoids, 28-thia-, 28-selena- and 28-tellura-2,7-naphthiporphyrin, have been studied. The open-aperture Z-scan technique was used to determine two-photon absorption cross-sections in the near infrared range using an amplified femtosecond laser system. The maximum values of the cross sections were found to be 99, 200 and 650 GM at 900 nm and 1, 13 and 31 GM at 1400 nm for the three investigated compounds, respectively. These results demonstrate enhanced 2PA properties compared with well-known porphyrin photosensitizers, such as Foscan®, showing the potential of porphyrin core modification for optimizing infrared nonlinear absorbers.

 Received 7th June 2022
 Accepted 15th June 2022

DOI: 10.1039/d2ra03167a

rsc.li/rsc-advances

Introduction

Carbaporphyrinoids are porphyrin analogues characterized by a presence of carbon atom(s) within the coordination cavity of the macrocycle.¹ This profound structural alteration of archetypical porphyrin framework results in systems providing an unusual coordination environment composed of nitrogen donors and carbon atoms capable of metal or metalloid binding.²

In this respect, the carbaporphyrinoids embedding polycyclic aromatic hydrocarbon (PAH) subunits, namely aceneporphyrinoids, were found to be particularly intriguing, as it was demonstrated that the PAH motif is a crucial factor dictating the overall properties of the hybrid molecule.^{3–5} The extent to which the electronic properties are altered depends on the nature of the PAH moiety present and whether it takes part in the π -delocalization with the rest of the macrocycle. In recent years aceneporphyrinoids have received a lot of attention due to their atypical π -conjugation,^{6,7} their aromaticity varying from nonaromatic to antiaromatic,^{8,9} and their ability to form stable organometallic complexes with metals of uncommon oxidation states.^{6,10–12} The incorporation of a particular PAH into the

macrocycle can be accomplished in a way that the cavity size exceeds 16 atoms, typical for a porphyrin/porphyrinoid of regular size.^{1,13,14} The resultant macrocycles are considered expanded carbaporphyrinoids.¹⁵

One selected type of a PAH embedded porphyrinoid is that of naphthiporphyrin. Up to date a series of its constitutional isomers have been synthesized, including 1,3-,^{16,17} 1,4-,^{16,18} 1,5-,¹⁹ and 1,7-naphthiporphyrinoids.⁴ These macrocycles contribute porphyrin-like donor atoms within the precisely designed cavity and are becoming more and more desirable for applications within organoelement chemistry and organometallic chemistry.^{2,20} The naphthiporphyrins have also been demonstrated to display exceptional conformational flexibility.^{21–23}

The molecular properties of carbaporphyrinoids can be further altered by the incorporation of heteroatoms^{24–26} such as O, S, Se, or Te within the macrocyclic cavity. In most cases, the modification significantly affects the electronic properties of the molecule, which in turn changes the spectral, structural, and coordination properties.^{3,5,27}

In a previous study, a new constitutional isomer of naphthiporphyrin was designed and synthesized, namely 28-hetero-2,7-naphthiporphyrin.²⁸ The compound was proven to act as a macrocyclic ligand, as demonstrated by the formation of organophosphorus(v) complexes.

It has been well established that two-photon absorption (2PA) properties are affected by both structural and electronic properties of molecules, such as the extent of the π -conjugation length,^{29–34} and the planarity and aromaticity of the molecule.^{35–41} However, the photophysical properties for heteroporphyrins, and particularly carbaporphyrinoids, have not been

^aAdvanced Materials Engineering and Modelling Group, Faculty of Chemistry, Wrocław University of Science and Technology, Wybrzeże Wyspińskiego 27, 50-370 Wrocław, Poland. E-mail: katarzyna.matczyszyn@pwr.edu.pl

^bLaboratoire PEIRENE, Université de Limoges, 123 Avenue Albert Thomas, 87060 Limoges, France

^cDepartment of Chemistry, University of Wrocław, 14 F. Joliot-Curie St., 50-383 Wrocław, Poland. E-mail: bartosz.szyszko@chem.uni.wroc.pl

† Electronic supplementary information (ESI) available: Re and Im values of 1-S, 1-Se and 1-Te are available. See <https://doi.org/10.1039/d2ra03167a>



extensively studied despite their potential use in applications such as photodynamic therapy,⁴² sensor development,⁴³ and as catalysts⁴⁴ and anion-binding agents.⁴⁵ Herein, we provide details on the 2PA properties, characterized using the Z-scan technique,^{46,47} of 28-hetero-2,7-naphthiopyrins differing in the presence of sulfur (**1-S**), selenium (**1-Se**) and tellurium (**1-Te**) atoms within the macrocyclic cavity (Fig. 1). To the best of our knowledge, these are some of the very few carbaporphyrinoids for which the nonlinear optical properties were measured using this technique.⁴⁸ Several examples of previous works describing the 2PA properties of atypical porphyrinoids include N-confused hexaphyrins,⁴⁹ expanded porphyrins such as cyclo[n]pyrrole, amethyrin and rubyrin,³⁹ and biradicaloid *meso*-substituted [26]hexaphyrin.⁵⁰

Results and discussion

One-photon absorption

The three investigated compounds **1-S**, **1-Se** and **1-Te** were dissolved in ultrapure dichloromethane to ensure no chemical changes of the molecules took place during the measurements. When dissolved, they formed dark green solutions. The UV-Vis spectra contained an intense Soret-like band located in the 347–358 nm range, as well as a second relatively intense band in the 443–452 nm range (see Fig. 2).

They also display a broad absorption band extending through the 500–850 nm range, with maxima at 661 nm for **1-S**, 670 nm for **1-Se** (for both 0.5 and 1%) and 679 nm for **1-Te**. These bands and spectral patterns are characteristics of nonaromatic carbaporphyrinoids.³⁶ As the heterocyclic ring D is varied in the macrocycles from thiophene to selenophene to tellurophene (Fig. 1), the absorption bands display a modest bathochromic (red) shift. This observed red-shift is a common effect and has been well-documented for heteroporphyrins⁵¹ and heterocarborporphyrinoids,^{19,28} likely due to the increasing metallic nature and electron delocalization of group 16 elements (the chalcogens).⁵² Due to the differing sizes of the heteroatoms in the 28th position, the conformation of the macrocycle is affected, and may also have some effect on the photophysical properties, due to changes in aromaticity and π -electron delocalization.⁵³

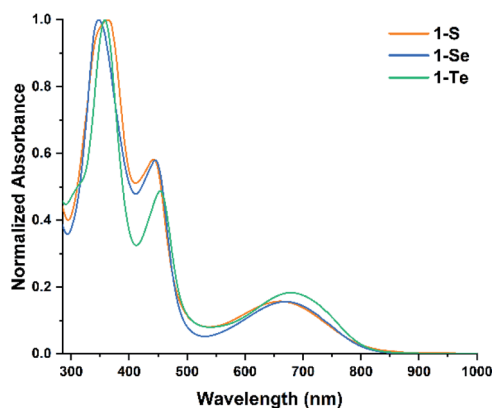


Fig. 2 UV-Vis absorption spectra of **1-S** (concentration = 1% w/w), **1-Se** (concentration = 1% w/w) and **1-Te** (concentration = 0.5% w/w) measured in DCM.

Two-photon absorption

Changing the heterocyclic ring D from thiophene to selenophene to tellurophene, leads to changes in the electron delocalizability and charge transfer of the molecules, due to the differences of the three heteroatoms with tellurium being the heaviest and less electronegative than selenium and sulfur.⁵⁴ The presence of these heavy atoms not only red-shifts the 1PA band, but has also been known to enhance the intersystem crossing (ISC) of a molecule.^{55–57} Since 2PA, a third-order nonlinear optical phenomenon, is known to be influenced by charge transfer efficiency^{58,59} which is related to electron donor properties, we have compared the 2PA cross-section (σ_2) values of **1-S**, **1-Se** and **1-Te** by using the femtosecond open-aperture Z-scan technique.^{60–62} In order to determine the maximum σ_2 values for these compounds, we have measured the two-photon absorption at excitation wavelengths in the ranges corresponding to the doubled wavelength region of the 1PA bands, where the one-photon absorption contribution to the open aperture signal (which may be due to the excited state absorption process and/or absorption saturation) could be manageable, between 850 and 1600 nm for **1-S_1**, **1-Se_1**, and **1-Te_0.5**, and between 800 and 1600 nm for **1-Se_0.5**. The 2PA cross-sections (σ_2), which are a measure of the probability of simultaneous absorption of two photons by a molecule were computed and the values are presented in Fig. 3 alongside the

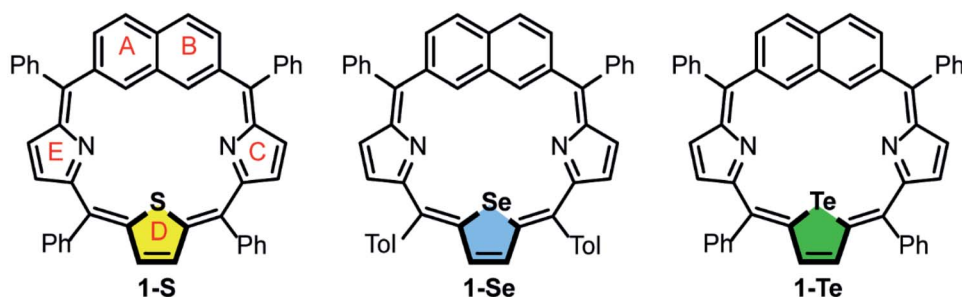


Fig. 1 Structures of **1-S**, **1-Se** and **1-Te**.

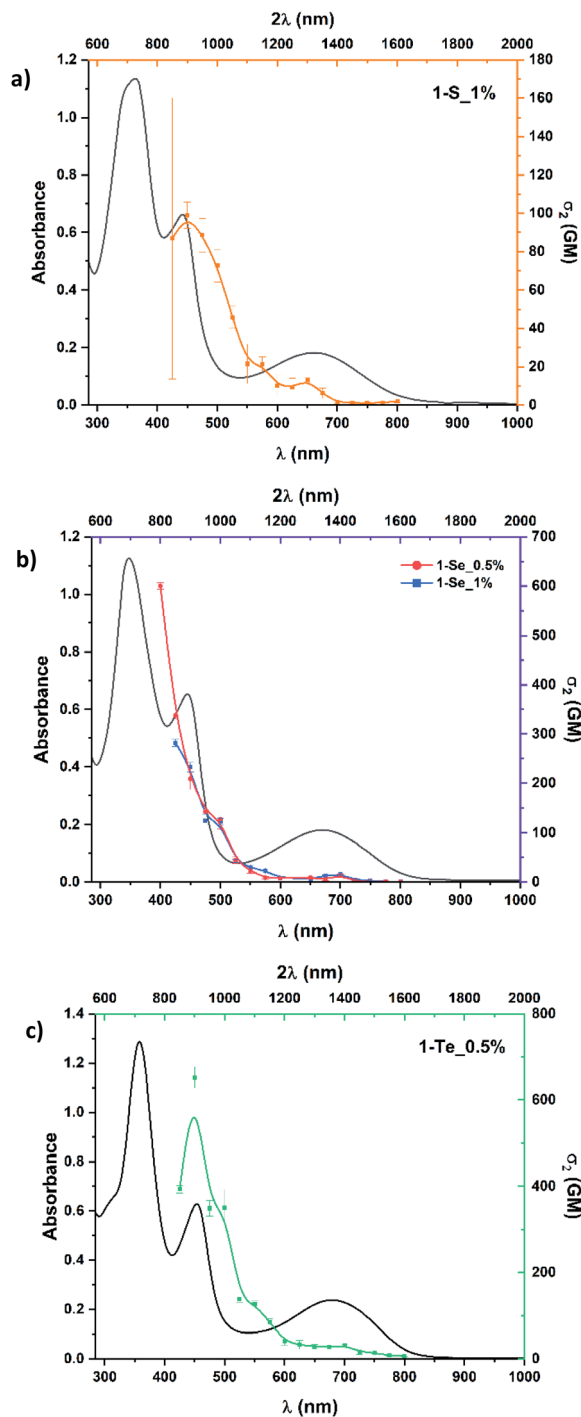


Fig. 3 Overlay of one- (black solid line) and two-photon absorption spectra for 1-S_1 (a), 1-Se_0.5 and 1-Se_1 (b) and 1-Te (c) in DCM. The two-photon absorption cross-sections are derived from open aperture Z-scan measurements and the one-photon spectra are plotted against twice the wavelength (2λ).

one-photon spectra plotted against the doubled wavelength. This way of presenting the 2PA data rests on the assumption that the same excited states can be reachable by both 1PA and 2PA, which is a normal occurrence for non-centrosymmetric molecules.⁶³ One should note, however, that the relative 2PA

strengths of various absorption bands do not have to follow the patterns seen in 1PA spectra.

The examples of open aperture Z-scan curves are displayed below for two wavelengths, 900 and 1400 nm, which are at approximately twice the wavelengths of 1PA peaks (Fig. 4 and Table 1). It is evident that the 1-S and 1-Se display weaker nonlinear absorption compared to that of 1-Te, with the nonlinear absorption being almost indiscernible for 1-S at 1400 nm. As expected, the two differently concentrated solutions of 1-Se complex (0.5% and 1%) exhibit the nonlinear absorption that roughly scales with the concentration, thus, as seen in Table 1, the cross sections calculated from those data are in agreement.

Examination of the data indicates that all compounds show a relatively weak TPA maximum at around 1400 nm with the value of σ_2 being about twice higher for 1-Te compared to 1-Se, and about 6 times higher when compared to 1-S. One does expect that shorter wavelength maxima may appear at around 700 and 900 nm. This, however, cannot be determined rigorously because of the overlap of those ranges with the tail of the 1PA absorption. The presence of the band at around 900 nm can be invoked as the existence of a knee-like feature in all two-photon spectra.⁶⁴ The increase of σ_2 to 600 GM at 800 nm for 1-Se is likely to arise from the presence of excited state absorption. The 1PA contribution is probably still too high at 800 nm, leading to the observed increase in calculated 2PA cross-section value due to excited state absorption or absorption saturation. The cross sections determined here exceed 650 GM for 1-Te. Still larger cross-sections may be present at shorter

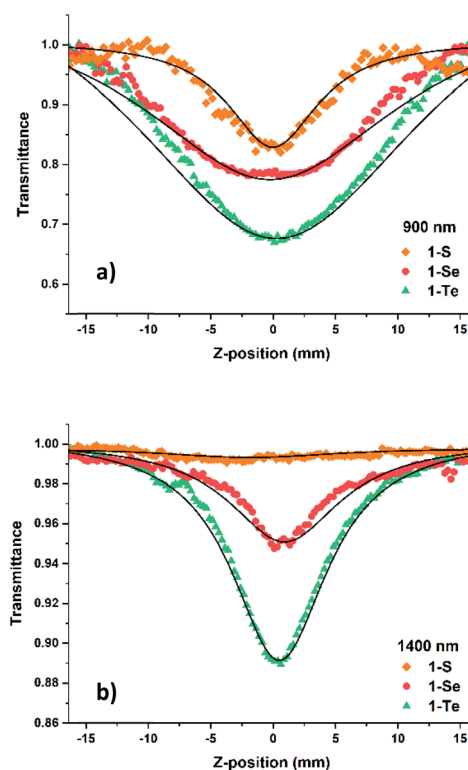


Fig. 4 Open aperture Z-scan curves of samples 1-S, 1-Se_0.5 and 1-Te at 900 nm (a) and 1400 nm (b).



Paper

Table 1 The calculated two-photon absorption cross-section values of the investigated compounds in DCM (MW represents molecular weight)

Sample	2PA λ (nm)	σ_2 (GM)	σ_2 /MW (GM g ⁻¹)
1-S_1	900	99 ± 6.8	0.143
	1400	1.4 ± 0.8	0.002
1-Se_0.5	900	209 ± 22	0.272
	1400	13.2 ± 3	0.017
1-Se_1	900	233 ± 10	0.303
	1400	15.7 ± 1.5	0.020
1-Te_0.5	900	652 ± 25	0.826
	1400	31.5 ± 3	0.040

wavelengths, but the evidence for that is hard to obtain because of the influence of 1PA.⁶⁵

From the results presented above, we can further support the fact that changing from sulfur to selenium, and to the heavier tellurium atom, yields larger 2PA cross-sections. There is increased electron density at the center of these heavy atoms,^{66–69} which has been interpreted to be due to the increased electron donation down the chalcogen family because of the decreased electronegativity of each element. This may lead to improved charge transfer⁷⁰ and thus, lead to increased 2PA cross-sections. Further studies of photophysical properties of each compound would be helpful to confirm this mechanism. Such studies may shed more light on the role of electron donation and the heavy atom effect, which also promotes intersystem crossing due to atoms with large atomic numbers being able to induce strong spin–orbit coupling (SOC).^{56,71,72} The heavy atom effect has been shown to cause changes to photophysical properties,^{73–76} observed here by the increasing 2PA cross-section as the heavy atom becomes heavier. Both effects being of great interest for novel materials for related photochemical and photophysical applications, such as photodynamic therapy,^{77–79} optical limiting,^{80–82} optical data storage,^{83,84} 2PA imaging,^{85,86} microfabrication,^{87,88} and more.

While the main interest in the present study has been in nonlinear absorption properties of the investigated molecules, the closed-aperture Z-scan measurements on their solutions in principle allow for the determination of both the nonlinear absorptive and refractive properties. These are most often presented as the real (Re(γ)) and imaginary (Im(γ)) parts of the cubic hyperpolarizability (γ) of the studied compounds.^{89–91}

Fig. 5 shows the spectra of the complex hyperpolarizability, γ ($-\omega; \omega, -\omega, \omega$) that were derived from the Z-scan measurements. For all three compounds the absolute values of the real and imaginary parts of γ are of the order of 10^{-33} esu. While the imaginary part is related to the two-photon cross section and its dispersion follows that of the spectral dependence of σ_2 , on the other hand, the real part appears to be negative in almost the whole spectral region investigated which is typical for compounds with strong two-photon absorption. One may note that, thanks to relatively high concentrations of the solutions, the solute contribution to the total refractive nonlinearity of the solution was relatively high leading to acceptably low errors in the determination of Re(γ). As the chalcogen changes from S to

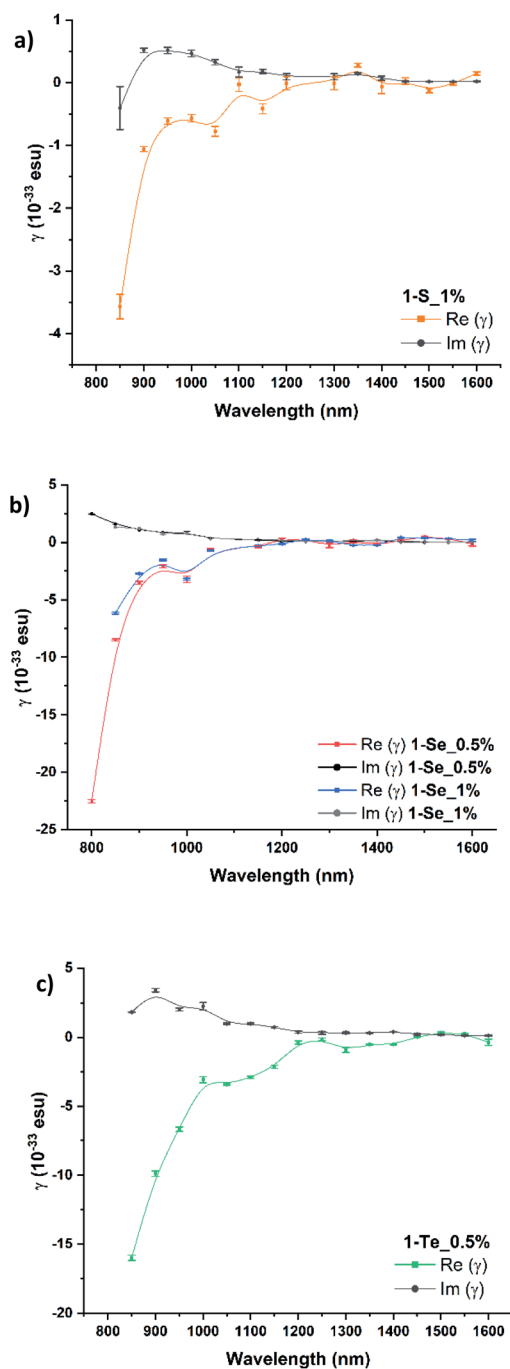


Fig. 5 Spectra of the real and imaginary parts of the hyperpolarizability γ , derived from the Z-scan measurements for samples 1-S_1 (a), 1-Se_0.5 and 1-Se_1 (b) and 1-Te_0.5 (c).

Se to Te, we see an increase in the hyperpolarizability (γ) value. Previous studies suggest that the heavier heteroatom is responsible for decreases in the transition energy between the ground and excited state involved in the transition that contributes to γ .^{92,93} Thus, this change in transition energy may also lead to the enhanced 2PA cross-sections observed as we move down the chalcogen group.

The measured 2PA cross-sections, for 1-Te in particular, show a marked improvement upon traditional macrocyclic



molecules. The distinct advantage of these compounds is their ability to absorb at much longer wavelengths (1400 nm) compared to commonly used porphyrins, Foscan® (652 nm) and meso-tetra-4-hydroxyphenylporphyrin (648 nm),⁹⁴ for the treatment of head and neck cancers, demonstrating their potential for future applications.

Experimental

Solvents were obtained commercially and used without purification.

Synthesis

1-S, **1-Se**, and **1-Te** were synthesized as described earlier.²⁸

UV-Vis

All UV-Vis spectra were recorded on a JASCO V-730 spectrophotometer.

Z-scan

The two-photon absorption properties have been determined using the Z-scan technique.⁹⁵ The experiments were performed over a wide range of wavelengths (800–1600 nm), achieved by employing an Astrella Ti : Sapphire amplifier (output wavelength 800 nm) pumping a TOPAS Prime optical parametric amplifier equipped with a NirUVis frequency mixer, which delivered wavelength tunable pulses with a duration of about 50 fs and the repetition rate of 1 kHz. The output beam was selected with a polarization separator and attenuated using neutral density filters. DCM solutions of **1-S**_1, **1-Se**_0.5, **1-Se**_1 and **1-Te**_0.5 were placed in stoppered 1 mm glass cuvettes. Two different concentrations of solutions were studied for **1-Se**: 0.5% (**1-Se**_0.5) and 1% (**1-Se**_1) w/w while the concentration of **1-S** was 1% w/w, and **1-Te** was 0.5% w/w. In a Z-scan experiment the sample is moved along the axis of the incident beam (z-direction), prior to and past the focal point, and the so-called open and closed aperture signals are recorded: corresponding to the overall transmittance of the sample and that of the central part of the beam as selected by an aperture in the far field, respectively. These signals, as well as the signal corresponding to the incident beam, were viewed on an oscilloscope and digitized and transferred to a computer *via* a National Instruments BNC-2110 Terminal Block and National Instruments PCI-6143 Multifunction I/O Device. The obtained results for the three compounds were calibrated by using Z-scan measurements performed on a fused silica plate, for which the nonlinear refractive index was assumed employing literature data and compared with measurements of an identical glass cuvette filled solely with the solvent.^{96–98} The obtained data were analyzed using a custom fitting program that utilised equations derived by Sheik-Bahae, *et al.*⁶⁰

Conclusions and outlook

The investigation of one- and two-photon absorption properties of expanded heteroporphyrins **1-S**, **1-Se** and **1-Te** demonstrates

an improvement upon well-known porphyrin photosensitizers used *e.g.*, in photodynamic therapy. While the measured 2PA cross-sections may appear moderate in comparison to much larger molecules investigated in this context, it is important that reasonable values can be obtained even at the relatively long wavelength of 1400 nm and order of magnitude higher values are seen at 900 nm for **1-Se** and **1-Te**, exceeding values for well-known PDT photosensitizers such as Foscan®, which has $\sigma_2 = 28 \pm 8$ GM, in DMSO at 775 nm.⁹⁹

Further investigations would be required to determine whether the modification of the porphyrinoid core can be utilized to build more extended porphyrin-like systems with sizeable enhanced 2PA properties.

Author contributions

Conceptualization: B. S. and K. M.; formal analysis: E.R.; funding acquisition: M. S., B. S. and K. M.; investigation: E. R. and R. D.; supervision: K. M.; validation: K. S., M. S., L. L. G. and B. S.; visualization: E. R., R. D., K. S., M. S., L. L. G., B. S. and K. M.; writing – original draft: E. R.; writing – review & editing: E. R., K. S., M. S., L. L. G., B. S., and K. M.

Conflicts of interest

There are no conflicts to declare.

Acknowledgements

This work was financially supported by the European Union's Horizon 2020 research and innovation programme under the Marie Skłodowska-Curie grant (agreement no. 764837). The work at the University of Wrocław was funded by National Science Centre of Poland (2017/26/D/ST5/00184). MS and RD acknowledge the NCN Harmonia grant 2016/22/M/ST4/00275. KM and MD thanks National Science Centre of Poland for the grant no. 2019/35/B/ST4/03280.

References

- 1 T. D. Lash, *Chem. Rev.*, 2017, **117**, 2313–2446.
- 2 B. Szyszko and L. Latos-Grażyński, *Chem. Soc. Rev.*, 2015, **44**, 3588–3616.
- 3 K. Laxman, A. Kumar and M. Ravikanth, *Asian J. Org. Chem.*, 2020, **9**, 162–180.
- 4 J.-H. Hong, A. S. Aslam, M. Ishida, S. Mori, H. Furuta and D.-G. Cho, *J. Am. Chem. Soc.*, 2016, **138**, 4992–4995.
- 5 A. Sinha and M. Ravikanth, *J. Org. Chem.*, 2021, **86**, 6100–6110.
- 6 B. Szyszko, L. Latos-Grażyński and L. Sztrenberg, *Chem. Commun.*, 2012, **48**, 5004–5006.
- 7 B. Szyszko, P. Rymut, M. Matviyishyn, A. Białońska and L. Latos-Grażyński, *Angew. Chem., Int. Ed.*, 2020, **59**, 20137–20146.
- 8 M.-C. Yoon, S. Cho, M. Suzuki, A. Osuka and D. Kim, *J. Am. Chem. Soc.*, 2009, **131**, 7360–7367.
- 9 T. Tanaka and A. Osuka, *Chem. Rev.*, 2017, **117**, 2584–2640.



- 57 K. M. Farrell, M. M. Brister, M. Pittelkow, T. I. Sølling and C. E. Crespo-Hernández, *J. Am. Chem. Soc.*, 2018, **140**, 11214–11218.
- 58 B. Küçüköz, G. Sevinç, E. Yildiz, A. Karatay, F. Zhong, H. Yılmaz, Y. Tutel, M. Hayvalı, J. Zhao and H. Yaglioglu, *Phys. Chem. Chem. Phys.*, 2016, **18**, 13546–13553.
- 59 S. Tekin, B. Küçüköz, H. Yılmaz, G. Sevinç, M. Hayvalı, H. G. Yaglioglu and A. Elmali, *J. Photochem. Photobiol., A*, 2013, **256**, 23–28.
- 60 M. Sheik-Bahae, A. A. Said, T.-H. Wei, Y.-Y. Wu, D. J. Hagan, M. Soileau and E. W. Van Stryland, *Sensitive measurement of optical nonlinearities using a single beam*, San Diego, CA, 1989.
- 61 L. M. Mazur, T. Roland, S. Leroy-Lhez, V. Sol, M. Samoc, I. D. W. Samuel and K. Matczyszyn, *J. Phys. Chem. B*, 2019, **123**, 4271–4277.
- 62 E. W. Van Stryland and M. Sheik-Bahae, in *Characterization Techniques and Tabulations for Organic Nonlinear Materials*, Marcel Dekker, Inc, 1st edn, 1998, pp. 671–708.
- 63 M. Pawlicki, H. A. Collins, R. G. Denning and H. L. Anderson, *Angew. Chem., Int. Ed. Engl.*, 2009, **48**, 3244–3266.
- 64 S. J. Zelewski, K. C. Nawrot, A. Zak, M. Gladysiewicz, M. Nyk and R. Kudrawiec, *J. Phys. Chem. Lett.*, 2019, **10**, 3459–3464.
- 65 M. Drobizhev, N. Makarov, T. Hughes and A. Rebane, *J. Phys. Chem. B*, 2007, **111**, 14051–14054.
- 66 F. A. Devillanova and W.-W. Du Mont, *Handbook of chalcogen chemistry: new perspectives in sulfur, selenium and tellurium*, Royal Society of Chemistry, 2013.
- 67 W. Levason, S. D. Orchard and G. Reid, *Organometallics*, 1999, **18**, 1275–1280.
- 68 A. J. Barton, W. Levason and G. Reid, *J. Organomet. Chem.*, 1999, **579**, 235–242.
- 69 A. J. Genge, S. Orchard and S. A. Pope, *J. Chem. Soc., Dalton Trans.*, 1999, (14), 2343–2352.
- 70 H. Yılmaz, B. Küçüköz, G. Sevinç, S. Tekin, H. G. Yaglioglu, M. Hayvalı and A. Elmali, *Dyes Pigm.*, 2013, **99**, 979–985.
- 71 J. Zhao, W. Wu, J. Sun and S. Guo, *Chem. Soc. Rev.*, 2013, **42**, 5323–5351.
- 72 A. Rodriguez-Serrano, V. Rai-Constapel, M. C. Daza, M. Doerr and C. M. Marian, *Phys. Chem. Chem. Phys.*, 2015, **17**, 11350–11358.
- 73 A. Karatay, M. C. Miser, X. Cui, B. Küçüköz, H. Yılmaz, G. Sevinç, E. Akhüseyin, X. Wu, M. Hayvalı and H. G. Yaglioglu, *Dyes Pigm.*, 2015, **122**, 286–294.
- 74 B. Sauerwein and G. B. Schuster, *J. Phys. Chem.*, 1991, **95**, 1903–1906.
- 75 D. G. Hilmey, M. Abe, M. I. Nelen, C. E. Stilts, G. A. Baker, S. N. Baker, F. V. Bright, S. R. Davies, S. O. Gollnick and A. R. Oseroff, *J. Med. Chem.*, 2002, **45**, 449–461.
- 76 C.-L. Sun, Q. Liao, T. Li, J. Li, J.-Q. Jiang, Z.-Z. Xu, X.-D. Wang, R. Shen, D.-C. Bai and Q. Wang, *Chem. Sci.*, 2015, **6**, 761–769.
- 77 J. Bhawalkar, N. Kumar, C.-F. Zhao and P. Prasad, *Journal of Lasers in Medical Sciences*, 1997, **15**, 201–204.
- 78 S. Kim, T. Y. Ohulchanskyy, H. E. Pudavar, R. K. Pandey and P. N. Prasad, *J. Am. Chem. Soc.*, 2007, **129**, 2669–2675.
- 79 Q. Zheng, A. Bonoiu, T. Y. Ohulchanskyy, G. S. He and P. N. Prasad, *Mol. Pharm.*, 2008, **5**, 389–398.
- 80 J.-C. Liu, X.-Z. Li and Y. Zhang, *Two-photon absorption induced optical power limiting behaviour of strong femtosecond hyper-Gaussian pulses*, Beijing, China, 2016.
- 81 M. G. Silly, L. Porrès, O. Mongin, P.-A. Chollet and M. Blanchard-Desce, *Chem. Phys. Lett.*, 2003, **379**, 74–80.
- 82 Q. Zheng, S. K. Gupta, G. S. He, L. S. Tan and P. N. Prasad, *Adv. Funct. Mater.*, 2008, **18**, 2770–2779.
- 83 B. H. Cumpston, S. P. Ananthavel, S. Barlow, D. L. Dyer, J. E. Ehrlich, L. L. Erskine, A. A. Heikal, S. M. Kuebler, I. Y. S. Lee, D. McCord-Maughon, J. Qin, H. Röckel, M. Rumi, X.-L. Wu, S. R. Marder and J. W. Perry, *Nature*, 1999, **398**, 51–54.
- 84 Q. Zhang, S. Yue, H. Sun, X. Wang, X. Hao and S. An, *J. Mater. Chem. C*, 2017, **5**, 3838–3847.
- 85 Z. F. Chang, L. M. Jing, B. Chen, M. Zhang, X. Cai, J. J. Liu, Y. C. Ye, X. Lou, Z. Zhao, B. Liu, J. L. Wang and B. Z. Tang, *Chem. Sci.*, 2016, **7**, 4527–4536.
- 86 Q. Zhang, X. Tian, H. Zhou, J. Wu and Y. Tian, *Materials*, 2017, **10**, 223.
- 87 F. Niesler and M. Hermatschweiler, *Opt. Photonik*, 2016, **11**, 54–57.
- 88 E. Scarpa, E. D. Lemma, R. Fiammengo, M. P. Cipolla, F. Pisanello, F. Rizzi and M. De Vittorio, *Sens. Actuators, B*, 2019, **279**, 418–426.
- 89 Z. Pokladek, N. Ripoché, M. Betou, Y. Trolez, O. Mongin, J. Olesiak-Banska, K. Matczyszyn, M. Samoc, M. G. Humphrey and M. Blanchard-Desce, *Chem.-Eur. J.*, 2016, **22**, 10155–10167.
- 90 K. Matczyszyn, J. Olesiak-Banska, K. Nakatani, P. Yu, N. A. Murugan, R. Zalesny, A. Roztoczynska, J. Bednarska, W. Bartkowiak and J. Kongsted, *J. Phys. Chem. B*, 2015, **119**, 1515–1522.
- 91 L. Chen, R. Hu, J. Xu, S. Wang, X. Li, S. Li and G. Yang, *Spectrochim. Acta, Part A*, 2013, **105**, 577–581.
- 92 K. Kamada, T. Sugino, M. Ueda, K. Tawa, Y. Shimizu and K. Ohta, *Chem. Phys. Lett.*, 1999, **302**, 615–620.
- 93 K. Kamada, M. Ueda, T. Sakaguchi, K. Ohta and T. Fukumi, *J. Opt. Soc. Am.*, 1998, **15**, 838–845.
- 94 L. Ma, J. Moan and K. Berg, *Int. J. Cancer*, 1994, **57**, 883–888.
- 95 M. Dudek, N. Tarnowicz-Staniak, M. Deiana, Z. Pokladek, M. Samoć and K. Matczyszyn, *RSC Adv.*, 2020, **10**, 40489–40507.
- 96 J. Wang, M. Sheik-Bahae, A. A. Said, D. J. Hagan and E. W. Van Stryland, *J. Opt. Soc. Am. B*, 1994, **11**(6), 1009–1017.
- 97 R. DeSalvo, M. Sheik-Bahae, A. Said, D. J. Hagan and E. W. Van Stryland, *Opt. Lett.*, 1993, **18**, 194–196.
- 98 M. Sheik-Bahae, J. Wang, R. DeSalvo, D. Hagan and E. Van Stryland, *Opt. Lett.*, 1992, **17**, 258–260.
- 99 B. Hamed, T. von Haimberger, V. Kozich, A. Wiehe and K. Heyne, *J. Photochem. Photobiol., A*, 2014, **295**, 53–56.

